Astron. Astrophys. 318, 269–274 (1997)

ASTRONOMY AND ASTROPHYSICS

Equivalent width of Na I and K I lines and reddening

Ulisse Munari[1] **and Tomaž Zwitter**[2]

[1] Osservatorio Astronomico di Padova, Sede di Asiago, I-36032 Asiago (VI), Italy (e-Mail: munari@astras.pd.astro.it)
[2] University of Ljubljana, Department of Physics, Jadranska 19, 1000 Ljubljana, Slovenia (e-Mail: tomaz.zwitter@uni-lj.si)

Received 18 January 1996 / Accepted 26 June 1996

Abstract. The profile, radial velocity and equivalent width of the interstellar lines of Na I (5890.0, 5895.9 Å) and K I (7699.0 Å) have been obtained from Echelle+CCD observations at resolving power $\lambda/\triangle\lambda$ ∼16,500 for 32 O and early B stars suffering from a reddening between E_{B-V}=0.06 and 1.57. The data have been used to search for and calibrate a relation between equivalent width and reddening.

When the interstellar lines show a single and sharp component, useful relations to estimate reddening from equivalent widths have been derived. The relation for Na I is most sensitive in the range $0.0 \leq E_{B-V} \leq 0.4$, and the one for K I takes over at higher reddening. Good quality equivalent width measurements allow E_{B-V} to be estimated with an accuracy of about 0.05 mag.

For multi–component profiles of Na I and K I lines the estimate of reddening is more ambiguous with a general scatter of 0.15 mag. Close blends of multiple components allow only an estimate of an upper limit to E_{B-V}.

Key words: interstellar medium: atoms – interstellar medium: dust, extinction

1. Introduction

Photometric determination of reddening for non–trivial astronomical objects like interacting binaries is a model–dependent, well–educated guess. Accounting for reddening is however a necessity in most investigations and calibration of independent reddening tracers is obviously wanted. A natural choice are the resonant lines of ions like NaI, KI, CaI, CaII, TiII etc. which are abundant in the interstellar medium (cf. Münch 1968).

We are regularly securing Echelle + CCD spectra of symbiotic stars and cataclysmic variables for a number of long term investigations. In the symbiotic star spectra the usual high space velocity of these objects fully splits the stellar from interstellar lines, while the broadness of spectral features associated with accretion disks in cataclysmic variables makes recognition of sharp interstellar lines an easy task. We have been therefore interested in searching for and calibrating a relation between reddening and the equivalent widths of interstellar lines.

The presence, properties and use of interstellar lines has been a leghtly discussed topic in the literature since the pioneering works of Hartmann (1904), Plaskett and Pearce (1933), Eddington (1934) and Wilson and Merrill (1937). Reviews on the formation of interstellar lines and the theory of the curve of growth can be found, among others, in Spitzer (1948), Münch (1968) and Gray (1992). Large bodies of experimental data have been provided e.g. by Münch (1957), Hobbs (1969a, 1969b, 1974, 1978a, 1978b), Welsh et al. (1991), Bertin et al. (1993) and Sembach et al. (1993). The majority of the investigations published so far have been obtained at very high resolution ($\lambda/\triangle\lambda \geq$50,000) and concentrated on the local interstellar medium or toward regions of low interstellar density. Few observations have been obtained for objects with $E_{B-V} \geq 0.5$ mag.

To exemplify the type of data available in literature the equivalent width of the interstellar Na I D1 line is plotted in Fig. 1 against reddening using the measurements presented by Hobbs (1974) and Sembach et al. (1993). Hobbs' data have been obtained with a photoelectric, pressure–scanned spectrometer employing an interference filter and three Fabry–Perot interferometers for a resolving power of ∼600,000. Sembach et al. data come from the more conventional Coudé Auxiliary Telescope (CAT) and Coudé Echelle Spectrograph (CES) + CCD at ESO (Chile), operated at a resolving power of ∼60,000. The distributions of the targets in galactic latitude, longitude and distance from the Sun are compared in Fig. 2. Hobbs' data pertain to bright, nearby stars while Sembach et al. data map the interstellar gas toward regions of low density.

In spite of the large body of data published so far, a simple and direct search for a relation between reddening and equivalent width (W) has been quite a rare exercise and this could justify the use of rough relations that sometimes appear in literature (e.g. Barbon et al. 1990 adopted for Na I doublet the linear relation E_{B-V} = 0.25 × W (Å) over the whole range $0.0 \leq E_{B-V} \leq 1.0$). Previous studies concentrated mostly on investigating chemical abundances, depletion and physical conditions in the interstellar medium, its subdivision into a cloud

Send offprint requests to: U. Munari

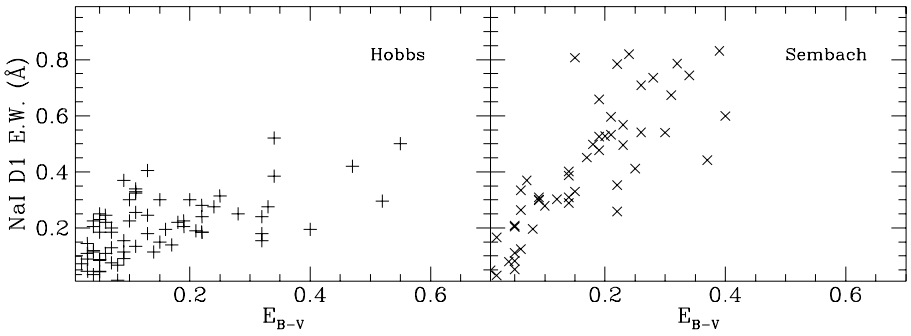

Fig. 1. Relation between equivalent width of the interstellar NaI D1 line and E_{B-V} for Hobbs (1969,1974) and Sembach et al. (1993) data sets.

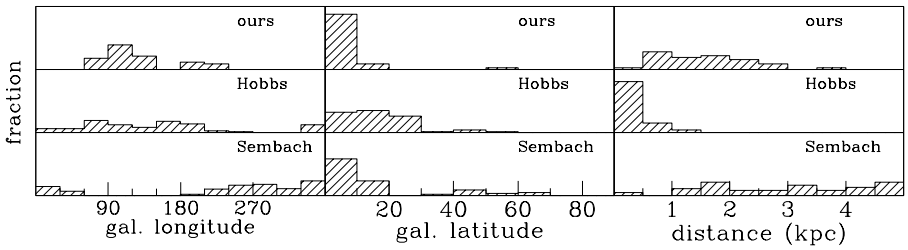

Fig. 2. Distribution in galactic longitude, latitude and distance of the stars observed in ours, Hobbs (1969,1974) and Sembach et al. (1993) surveys.

and an intercloud phase, and on the inferred Galactic kinematics (e.g. Pottasch 1972, Snow 1984, Sembach et al. 1993).

For these reasons and to investigate the whole matter at resolutions more typical of Cassegrain–fed Echelle spectrographs we have observed at a resolving power $\lambda/\triangle\lambda$ ∼16,500 the profile, radial velocity and equivalent width of the interstellar lines of Na I (5889.951, 5895.924 Å) and K I (7698.979 Å) for 32 O and B stars suffering from a reddening ranging between E_{B-V}=0.06 and 1.57. In this paper we discuss the results and the outcomes of the search for a usable relation between equivalent width and reddening.

2. Observations

The observations have been carried out with the Echelle spectrograph mounted at the Cassegrain focus of the 1.82 m telescope operated by Osservatorio Astronomico di Padova on top of Mt.Ekar in Asiago (Italy). The detector has been a THX31156 Thomson CCD 1024×1024 pixels, 19μm each and the slit was set to 2 arcsec. The whole λ range 5650–7850 Å was recorded on a single frame.

The dispersion for observations in Table 1 is 0.228 Å/pix at K I line, and 0.171 Å/pix at Na I doublet. The instrumental FWHM has been estimated from the mean of many thorium lines measured on all spectra to be 2.12 pixels for K I and 2.05 for Na I. The corresponding resolutions are $\lambda/\triangle\lambda$= 16,000 for K I and 17,000 for Na I.

Reduction of the spectra has been performed with the IRAF package and has included careful treatment of flat fielding. The zero point of the *spectrograph velocity* has been checked by measuring some of the numerous telluric lines around the K I and Na I lines and the sodium city lights recorded on *ad hoc* long exposures. The external accuracy of the reported radial velocities is of the order of 1 km sec^{-1}.

Light scattering along the dispersion direction tends to fill absorption lines and therefore to reduce their equivalent width. To estimate the light scattering along the dispersion we have studied the profile of strong, unblended and isolated thorium lines with varying slit width. We can confidently state from the quick and sharp drop to zero intensity outside line core that contribution from scattered light does not play a detectable role in our observations. The same result can be guessed by the very low intensity reached at the core of the strongest interstellar lines, where the recorded flux is only a few percent of the adjacent continuum (cf. Fig. 3).

Properties of the programme stars are given in Table 1. When the K I and Na I lines have been observed to split into multi–components, equivalent widths and radial velocities have been derived from deblending with multiple gaussians and are listed separately in Table 1, together with the equivalent width of the whole profile measured in the standard way. This and rounding–off of decimal figures accounts for the small differences between the whole profile equivalent width and the sum of equivalent widths of individual components.

The programme stars have been selected from the compilation of O and early B stars given by Sudzius and Bobinas (1994). Their values of E_{B-V} have been adopted (cf. Table 1). The selection criterion was to map the whole E_{B-V} range between 0.0 and 1.6 using the brightest stars observable at the time of our observing runs on Sept 8 and Dec 16, 1995. An additional night was originally planned for re–observations of stars already observed in other surveys of interstellar lines (to investigate the effect of varying resolving power), but cloudy sky prevented us from carrying out this part of the programme.

The distances in Table 1 have been computed assuming R_V=A_V/E_{B-V}=3.2, the absolute magnitude scale of Schmidt–Kaler (1982) and the mean V magnitude as listed by the SIMBAD database.

Table 1. Programme stars. For each star, the upper row refers to equivalent widths (in Å), the lower to heliocentric radial velocities (from Gaussian fitting to the lines) in km sec^{-1}. For objects with a single component profile, the data are listed in the column labelled 1^{st}. Columns labelled 2^{nd} and 3^{rd} are used for additional components in complex profile, while the equivalent width of the whole profile is listed in the column *All*. For stars HD 235825 and BD+60.493 the interstellar lines appeared as a blend of two components, however too close for a meaningful de–blending with Gaussian fitting.

Name	l^{II}	b^{II}	E_{B-V}	Dist.	Na I 5890.0 Å (D1)			Na I 5895.9 Å (D2)			K I 7699 Å		
				(kpc)	All	1^{st}	2^{nd}	all	1^{st}	2^{nd}	All	1^{st}	2^{nd}
HD 186980	67.4	+3.7	0.39	2.2		0.57			0.52			0.09	
						–11			–10				
HD 228779	73.2	–0.5	1.57	1.0		0.62			0.56			0.28	
						–10			–10				
HD 188891	75.5	+6.2	0.25	0.9		0.52			0.39			0.03	
						–16			–16				
HD 201345	78.4	–9.5	0.18	1.9		0.39			0.29			0.02	
						–13			–13				
HD 201638	80.3	–8.4	0.08			0.26			0.11			0.01	
						–10			–10				
HD 202349	82.6	–7.5	0.09	1.7		0.25			0.17			0.00	
						–12			–11				
HD 214652	95.7	–18.4	0.10	0.6		0.22			0.15			0.00	
						–9			–9				
HD 214680	96.7	–17.0	0.11	0.6		0.30			0.22			0.02	
						–11			–10				
HD 217101	100.1	–18.5	0.10	0.5		0.28			0.16			0.00	
						–6			–7				
HD 235825	102.9	–1.8	0.55	2.3	1.03			0.82					
HD 210478	104.5	+4.1	0.34	0.7		0.46			0.40			0.10	
						–15			–16				
HD 217086	110.2	+2.7	0.95	0.8		0.75			0.67			0.21	
						–17			–17				
HD 217035	110.3	+2.9	0.76	0.8		0.65			0.60			0.16	
						–16			–15				
HD 219287	110.8	–1.2	1.25	2.4	1.14	0.52	0.63	1.01	0.44	0.59			
						–14	–58		–13	–57			
HD 218342	111.4	+2.7	0.72	0.8		0.68			0.61			0.20	
						–17			–17				
BD +58.2580	111.5	–1.9	1.06	1.4	1.13	0.55	0.59	1.01	0.49	0.53	0.30	0.14	0.12
						–16	–53		–15	–53			
BD +59.2735	112.9	–1.4	1.40	1.9	1.17	0.55	0.65	1.06	0.46	0.61	0.37	0.16	0.15
						–10	–52		–10	–52			
HD 224257	115.3	–6.1	0.24	2.2	0.72	0.38	0.36	0.58	0.31	0.27		0.04	
						–14	–51		–15	–51			
BD +61.2559	116.3	+0.3	0.60	2.6	0.97	0.59	0.38	0.83	0.53	0.30		0.21	
						–18	–58		–18	–58			

3. Results

The equivalent width of a given absorption line is generally expressed as

$$W = \int [1 - \frac{I_\lambda}{I_\lambda(0)}]\ d\lambda = \int (1 - e^{-\tau_\lambda})\ d\lambda \qquad (1)$$

with the usual meaning of symbols. In the limit of very low optical depths the equivalent width becomes proportional to the column density of absorbing atoms along the line of sight. The latter is proportional to the column density of dust grains which cause the extinction, and therefore for low optical depths we may expect a linear relation $W \propto E_{B-V}$. In the limit of large optical depth the relation flattens to $W \propto \sqrt{ln\ \tau_0}$ where τ_0 is the optical depth at the line center: a large increase in the column density of absorbing atoms (and of reddening–inducing dust grains) does not change W appreciably. For a constant gas to dust ratio ($\tau_0 \propto E_{B-V}$) the general relation is (see e.g. Bowers & Deeming 1984):

$$W = \alpha \sum_{n=1}^{\infty} (-1)^{n-1} \frac{(\beta E_{B-V})^n}{n!\sqrt{n}} \qquad (2)$$

Table 1. Continued.

Name	l^{II}	b^{II}	E_{B-V}	Dist.	Na I 5890.0 Å (D1)				Na I 5895.9 Å (D2)				K I 7699 Å		
				(kpc)	All	1^{st}	2^{nd}	3^{rd}	All	1^{st}	2^{nd}	3^{rd}	All	1^{st}	2^{nd}
HD 13256	132.6	–0.6	1.38	1.7	1.01	0.72	0.31	0.89	0.67	0.24	0.36	0.28	0.09		
						–14	–52		–14	–53					
BD +59.451	133.5	–1.5	0.95	2.1	0.85	0.65	0.20		0.71	0.59	0.13			0.24	
						–12	–52			–12	–52				
BD +60.594	133.7	–1.3	0.67	2.0	0.73	0.58	0.16		0.65	0.53	0.14		0.34	0.27	0.08
						–14	–43			–13	–42				
BD +59.456	133.7	–1.3	0.83	1.8	0.89	0.66	0.25		0.75	0.64	0.13			0.24	
						–12	–50			–12	–53				
HD 13866	134.5	–4.2	0.38	2.6	0.93	0.63	0.32		0.77	0.58	0.21			0.15	
						–13	–50			–12	–50				
BD +60.493	134.6	+0.6	1.00	2.8	0.87				0.76					0.35	
HD 15785	135.3	+0.2	0.68	3.6	0.92	0.57	0.26	0.10	0.77	0.52	0.17	0.08		0.20	
						–10	–45	–72		–9	–45	–72			
HD 40111	184.0	+0.8	0.14	1.2		0.33				0.26				0.01	
						+15				+16					
HD 46966	205.8	–0.6	0.28	1.2		0.56				0.48				0.06	
						+20				+20					
HD 46149	206.2	–2.0	0.49	1.2		0.47				0.43				0.16	
						+22				+23					
HD 46202	206.3	–2.0	0.49	1.5		0.46				0.42				0.16	
						+23				+24					
HD 54439	225.4	–1.9	0.28	1.4		0.47				0.39				0.06	
						+26				+27					
HD 91316	234.9	+52.8	0.06	0.9	0.19	0.07	0.11		0.10	0.03	0.08			0.00	
						+19	–7			+20	–7				

Table 2. Empirical fit to the relation between E_{B-V} and the equivalent width of NaI D1 and KI 7699 Å lines for single lined absorption systems.

E_{B-V}	Equiv. width (Å)		E_{B-V}	Equiv. width (Å)	
	NaI D1	KI 7699		NaI D1	KI 7699
0.00	0.00	0.00	0.70	0.63	0.180
0.05	0.16	0.018	0.80	0.65	0.204
0.10	0.27	0.027	0.90	0.66	0.227
0.15	0.35	0.045	1.00	0.67	0.250
0.20	0.41	0.054	1.10	0.69	0.272
0.25	0.46	0.072	1.20	0.70	0.294
0.30	0.49	0.080	1.30	0.71	0.315
0.40	0.54	0.106	1.40	0.71	0.336
0.50	0.59	0.131	1.50	0.72	0.357
0.60	0.61	0.156	1.60	0.73	0.377

This sort of behaviour of W vs. E_{B-V} is well represented by the solid lines in Fig. 4, which are empirical fits to the data of the stars presenting a single component profile for the interstellar lines. The values of the coefficients α and β for the Na D1 and KI (7699 Å) lines from fit to our data are:

$$\begin{array}{lll} \text{Na D1:} & \alpha = 0.354 \pm 0.01 \text{ Å} & \beta = 11.0 \pm 1.0 \\ \text{K I:} & \alpha\beta = 0.277 \pm 0.01 \text{ Å} & \beta = 0.3 \pm 0.2 \end{array} \quad (3)$$

The errors are formal 2σ uncertainties. The large curvature of the Na D1 solution implies a slow convergence of the Eq. 2 series. For convenience sake the W vs. E_{B-V} relation is presented in numerical form in Table 2.

The star HD 228779 (the one with the highest reddening, E_{B-V}=1.57) probably lies behind a local dust pocket as suggested by its large extinction compared to stars HD 186980 and HD 201345, which appear at twice the distance along the same line of sight and which show interstellar lines at similar radial velocity. So the star HD 228779 was excluded from the above determination of α and β coefficients.

The weakest KI lines ($W < 0.05$Å) appear to have a systematically too low equivalent width in Fig. 4. This can be explained by uncertainties in line measurement and continuum fitting for such weak lines.

Accurate treatment of the line formation (including all relevant processes, constants, velocity distribution of absorbing atoms etc.) is given in the above cited references, and will not be repeated here. Hereafter we discuss only the use of multi-component Na I and K I lines in determination of reddening.

Most spectra with $W_{NaD1} > 0.7$Å or $W_{K\ I} > 0.15$Å show Na D1 and K I with double or multiple components separated by ≈ 40 km sec^{-1}. The profile of each component is however not resolved. Its FWHM is essentially the instrumental PSF of the Asiago Echelle spectrograph (18 and 19 km sec^{-1} respectively for Na I and K I in our survey). So it is appropriate to determine the equivalent width of each component by multiple Gaussian fitting.

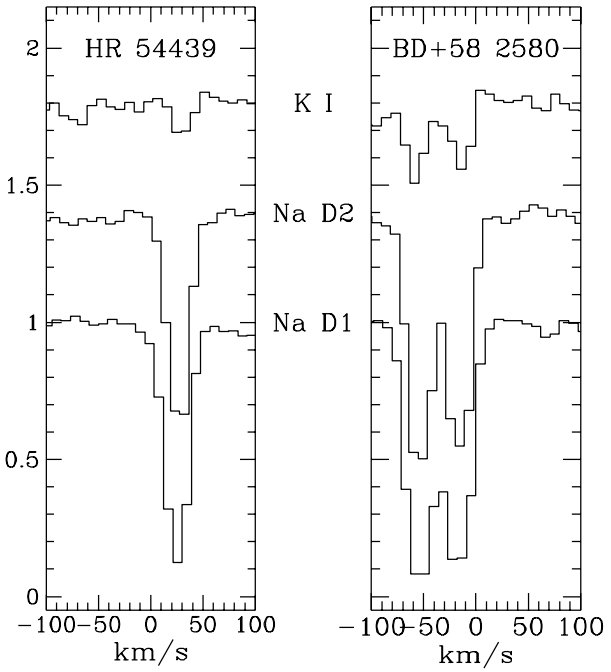

Fig. 3. Examples of the normalized spectra in the region of Na I and K I lines. The spectra have been vertically offset for clarity. Velocity is heliocentric.

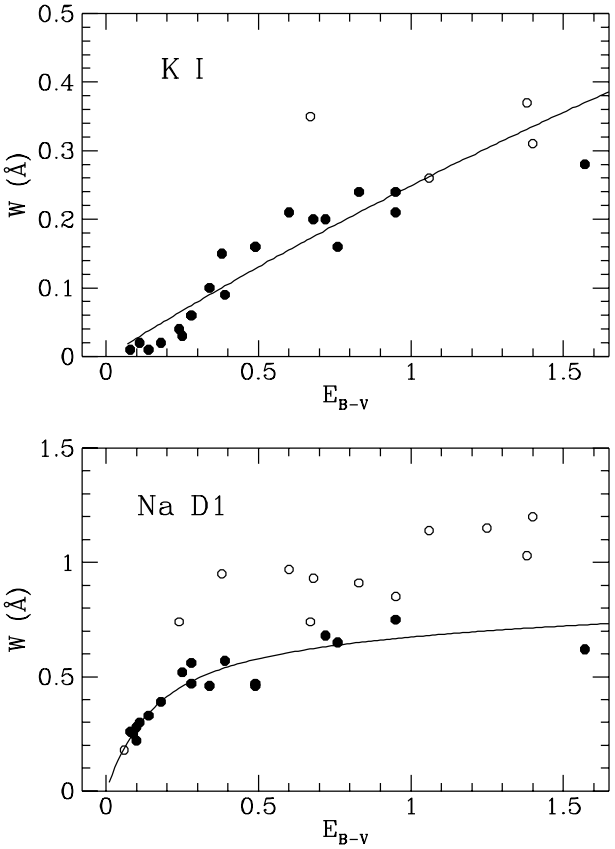

Fig. 4. Relation between equivalent width and reddening for the stars in our sample. *Filled circles* = single lined systems, *open circles* = multi–component line systems. Solid lines are best fits to the single lined systems as given by Eqs. 2 and 3 (see text).

The total equivalent width of the multiple component lines does not follow the solution for single components given by solid line in Fig. 4. The single component solution is steeper for lower W so it is natural that open circles of the multiple component objects in Fig. 4 lie above the solid line. The solid line can in fact serve as a lower limit to the expected W of the object if its E_{B-V} is known, or as an upper limit to E_{B-V} if W is measured.

The idea that a multiple-component profile is an ensemble of single components can be used further to check the single component solution given by Eqs. 2 and 3. Equivalent width of each component measured by Gaussian fitting is compared against the single component solution and translated into an expected contribution to the reddening. The reddening is additive so we can get the expected total reddening of the multiple-component profile this way. This can be obviously compared to the actual observed reddening. In Fig. 5 the difference between the expected and the observed reddening is plotted for the stars with single and with multiple component interstellar lines. The match is satisfactory without any obvious trends. In few cases the expected reddening is too high, possibly because there are multiple components not detected at our resolving power. The outlaying point on the right is due to anomalous reddening of HD 228779 discussed above. In the remaining 95% of the stars the reddening can be judged with a standard deviation of 0.15 magnitude from the equivalent width of the Na D1 or the K I line.

Equivalent widths of Na D1 and Na D2 lines are not independent. In turn one can use the D2 line to reduce uncertainty of the D1 line measurements and the reddening determination discussed above. The ratio of the oscillatory strengths for the two sodium lines is

$$\frac{3^2S_{1/2} - 3^2P^0_{3/2}\ (5889.951\ \text{Å})}{3^2S_{1/2} - 3^2P^0_{1/2}\ (5895.924\ \text{Å})} = \frac{0.631}{0.318} = 2.0 \qquad (4)$$

We studied the behaviour of this ratio vs. reddening for Hobbs, Sembach et al. and our data sets. The value of 2 is approached only at the lowest optical depths, and with increasing reddening the ratio asymptotically converges toward 1.1. Higher reddening generally means larger distances and therefore higher sensitivity to differential galactic rotation. The corresponding red–shifts account for the lowering of the above ratio toward 1.1, as thoroughly discussed by Wilson and Merrill (1937). It may be worth noticing that the effect becomes more and more pronounced if one compares Hobbs', Sembach et al. and finally our data sets. This agrees with the picture presented above as the Hobbs sample has the lowest and ours the highest fraction of low galactic latitude stars, so that our sample is most closely mapping the galactic rotation.

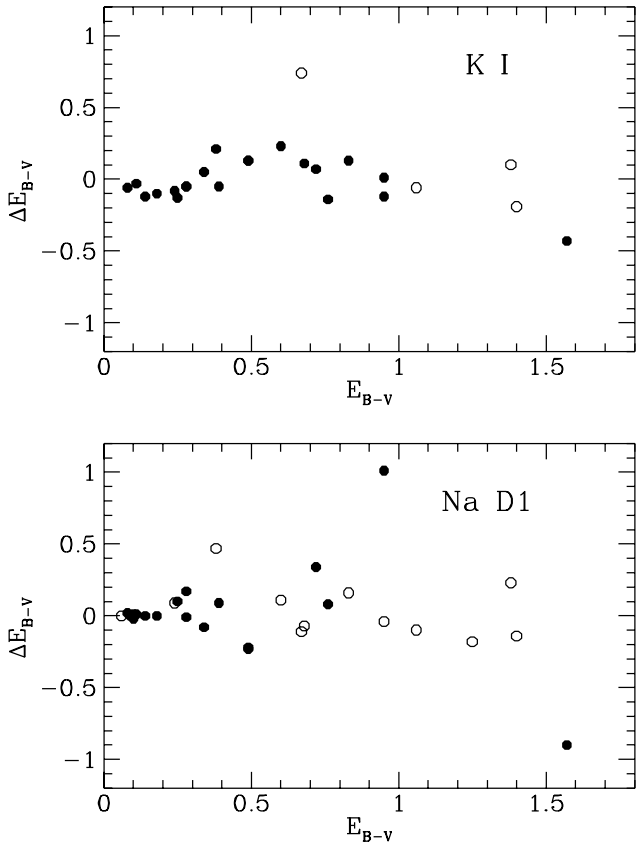

Fig. 5. The difference ΔE_{B-V} between the expected reddening, determined by Eqs. 2 and 3, and the observed one. *Filled circles* = single lined systems, *open circles* = multi–component line systems.

4. Discussion

We find that Eqs. 2 and 3 give a useful relation between the equivalent width of the Na D1 or the K I 7699 Å line and reddening for observations performed at resolutions typical of Cassegrain-fed spectrographs.

Generally the reddening can be estimated to within 0.15 magnitude. The relation is best determined at low values of E_{B-V} for the Na I lines. If the equivalent width of Na D1 line is below 0.5 Å, the reddening can be judged to within ∼0.05 mag. When NaD lines start to saturate (for $E_{B-V} \geq$0.4) the much weaker K I line can be profitably used. Even at the largest values of E_{B-V} here explored the equivalent width of K I line is still on the almost linear rise.

When the interstellar line profiles appear complex (particularly when one of the components is saturated) or the observed FWHM suggests close blending of unresolved multiple components, only an upper limit for E_{B-V} can be derived from observations. In case of dense dust pockets the strength of interstellar lines does not follow the increase of the reddening, so that E_{B-V} can be seriously underestimated. These anomalous cases however appear to be rare. For only $\sim$ 5% of objects in our sample the reddening from interstellar lines appears mis-judged by more than 0.5 mag.

The relation between equivalent width and reddening is consistent with the data set of Sembach et al. (1993). Widely scattered points with $0.2 < E_{B-V} < 0.4$ in Fig. 1 belong to multiple components similar to our data set (open circles in Fig. 3). Hobbs (1974) data in Fig. 1 deviate from the relation satisfied by our and Sembach et al. observations. This may be explained by the observing technique used by Hobbs (possible mis-judgment of the level of the adjacent continuum), coupled with the different selection criteria of observed stars.

In conclusion, interstellar lines are a useful tool to estimate the reddening as long as the spread in radial velocity of the absorbing medium (diffuse or locked into individual clouds) does not exceed the intrinsic velocity widths of the lines. As long as the gas/dust ratio, distribution of grain size and chemical abundances reflect the general interstellar medium, the same relation should apply also for cold circumstellar absorbing cocoons.

Acknowledgements. We thank the anonymous referee for useful comments. One of us (T.Z.) acknowledges partial financial support from the European Community CEE grant (contract no. ERBCIPDCT940028).

References

Barbon R., Benetti S., Cappellaro E., Rosino L., Turatto M. 1990, A&A 237, 79
Bertin P., Lallement R., Ferlet R., Vidal-Madjar A. 1993, A&A 278, 549
Bowers R.L., Deeming T. 1984, Astrophysics, Vol. 1, (Jones and Bartlett Publ., Boston), pag. 136
Eddington A.S. 1934, MNRAS 95, 2
Gray D.F. *The observation and analysis of stellar photospheres*, Cambridge Univ. Press
Hartmann J. 1904, ApJ 19, 268
Hobbs L.M. 1969a, ApJ 157, 135
Hobbs L.M. 1969b, ApJ 157, 165
Hobbs L.M. 1974, ApJ 191, 381
Hobbs L.M. 1978a, ApJ 222, 491
Hobbs L.M. 1978b, ApJS 38, 129
Münch G. 1957, ApJ 125, 42
Münch G. 1968, in *"Stars and Stellar Systems. VII. Nebulae and Interstellar Matter*, Middlehurst B.M. and Aller L.H. eds., Univ. of Chicago Press, pag. 365
Plaskett J.S., Pearce J.A. 1933, Pub.Dom.Ap.Obs.Victoria 5, 167
Pottasch S.R. 1972, A&A 17, 128
Schmidt–Kaler, Th. 1982, in Landolt/Bornstein, *Numerical Data and Functional Relationships in Science and Technology*, K.Schaifer and H.H.Voigt eds., New Series, Group IV, Vol. 2(b) (Springer, Berlin), pag.14
Sembach K.R., Danks A.C., Savage B.D. 1993, A&AS 100, 107
Snow T.P. 1984, ApJ 287, 238
Spietzer L. 1948, ApJ 108, 276
Sudzius J., Bobinas V. 1994, Baltic Astron. 3, 158
Welsh B.Y., Vedder P.W., Vallerga J.V., Craig N. 1991, ApJ 381, 462
Wilson O.C., Merrill P.W., 1937 ApJ 86, 44

This article was processed by the author using Springer-Verlag LaTeX A&A style file *L-AA* version 3.